

Radiatively Induced Neutrino Mass Model with Flavor Dependent Gauge Symmetry

SangJong Lee,¹ Takaaki Nomura,^{1,*} and Hiroshi Okada^{2,†}

¹*School of Physics, KIAS, Seoul 02455, Korea*

²*Physics Division, National Center for Theoretical Sciences, Hsinchu, Taiwan 300*

(Dated: December 3, 2024)

Abstract

We study an predictive radiative seesaw model at one-loop level with a flavor dependent gauge symmetry $U(1)_{\mu-\tau}$, in which we consider bosonic dark matter. We obtain a specific two zero texture with inverse mass matrix that provides us several predictions such as a specific pattern of Dirac CP phase. We also analyze the constraint of lepton flavor violations, muon $g-2$, relic density of dark matter, and collider physics, have numerical analysis and show allowed region to satisfy all the constraints.

Keywords:

*Electronic address: nomura@kias.re.kr

†Electronic address: macokada3hiroshi@cts.nthu.edu.tw

I. INTRODUCTION

The observation of neutrino oscillation confirms at least two non-zero masses of active neutrinos indicating physics beyond the standard model (SM) to generate the neutrino masses. Radiative seesaw models are one of the attractive candidate to generate the neutrino masses where a neutrino mass matrix is induced at loop level and a dark matter (DM) candidate can be included as a particle propagating inside a loop diagram for generating neutrino mass. It is also interesting to include flavor dependent gauge symmetry with which we can obtain predictive structure of neutrino mass matrix [1, 2].

One of the interesting flavor dependent $U(1)$ gauge symmetry is the $U(1)_{\mu-\tau}$ which can induce sizable deviation of muon anomalous magnetic dipole moment from SM prediction, Δa_μ , where experimental observation indicates $\Delta a_\mu \simeq O(10^{-9})$ suggesting discrepancy from the SM value. In addition, some interesting phenomenologies regarding the $U(1)_{\mu-\tau}$ are investigated, e.g. in Refs. [3–16]. We then apply the $U(1)_{\mu-\tau}$ gauge symmetry in a radiative seesaw model and investigate prediction in neutrino mass matrix.

In this paper, we construct a radiative seesaw model with $U(1)_{\mu-\tau}$ gauge symmetry and Z_2 symmetry in which we introduce exotic $SU(2)_L$ doublet leptons with $U(1)_{\mu-\tau}$, Z_2 even singlet scalar field, and Z_2 odd triplet and singlet scalar fields. In the model, active neutrino mass matrix is generated at one loop level where Z_2 odd particles propagate inside the loop. We find that structure of the Dirac mass matrix of exotic lepton determines that of the active neutrino mass matrix when exotic leptons have degenerated masses. In that case, we have two zero texture of the neutrino mass matrix which provides some predictions in neutrino oscillation experiments. In addition, we have DM candidate which is the lightest Z_2 odd neutral particle. Then we carry out numerical analysis taking into account charged lepton flavor violation (cLFV), Δa_μ , and relic density of DM searching for parameter region satisfying all the experimental constraints.

This paper is organized as follows. In Sec. II, we introduce our model and discuss some phenomenology such as neutrino mass matrix, lepton flavor violation, and some processes induced by Z' interactions. The numerical analysis is carried out in Sec. III to search for parameter region satisfying experimental constraints and to obtain some prediction for neutrino mass matrix. Finally we summarize the results in Sec. IV.

	Leptons								
Fermions	L_{Le}	$L_{L\mu}$	$L_{L\tau}$	e_R	μ_R	τ_R	L'_e	L'_μ	L'_τ
$SU(3)_C$	1	1	1	1	1	1	1	1	1
$SU(2)_L$	2	2	2	1	1	1	2	2	2
$U(1)_Y$	$-\frac{1}{2}$	$-\frac{1}{2}$	$-\frac{1}{2}$	-1	-1	-1	$-\frac{1}{2}$	$-\frac{1}{2}$	$-\frac{1}{2}$
$U(1)_{\mu-\tau}$	0	1	-1	0	1	-1	0	1	-1
Z_2	+	+	+	+	+	+	-	-	-

TABLE I: Field contents of fermions and their charge assignments under $SU(2)_L \times U(1)_Y \times U(1)_{\mu-\tau} \times Z_2$.

	VEV $\neq 0$		Inert	
Bosons	Φ	φ	Δ	S
$SU(2)_L$	2	1	3	1
$U(1)_Y$	$\frac{1}{2}$	0	1	0
$U(1)_{\mu-\tau}$	0	1	0	0
Z_2	+	+	-	-

TABLE II: Field contents of bosons and their charge assignments under $SU(2)_L \times U(1)_Y \times U(1)' \times Z_2$, where $SU(3)_C$ singlet for all bosons.

II. MODEL, PARTICLE PROPERTIES AND PHENOMENOLOGY

In this section, we introduce our model and discuss some phenomenology. As extra symmetries, local $U(1)_{\mu-\tau}$ and discrete Z_2 symmetries are added. In the fermion sector, we introduce $SU(2)_L$ doublet vector like fermions $L'_{e,\mu,\tau} \equiv [N, E]_{e,\mu,\tau}^T$, and impose a flavor dependent gauge symmetry $U(1)_{\mu-\tau}$ as summarized in Table I. Also Z_2 odd parity is imposed for this new fermion in order to discriminate the SM model leptons with $SU(2)_L$ and forbid the mixing between them.¹ In the scalar sector, we add an $SU(2)_L$ triplet inert scalar Δ real singlet inert scalar S , and singlet scalar φ to the SM Higgs Φ as summarized in

¹ Notice here that the neutral component of L' cannot be a DM candidate, because it is ruled out by the direct detection search via Z boson portal.

Table II. Notice here the Higgs doublet Φ (that spontaneously breaks electroweak symmetry), the $SU(2)$ singlet field φ (that spontaneously break $U(1)_{\mu-\tau}$ symmetry), have the vacuum expectation values (VEVs), which are respectively symbolized by $v/\sqrt{2}$, $v'/\sqrt{2}$, and Z_2 odd parity is also imposed for the inert scalars Δ and S due to forbidding the tree level neutrino masses through VEVs. Therefore the lightest neutral scalar boson with Z_2 odd parity can be a DM candidate.

Yukawa interactions: Under these fields and symmetries, the renormalizable Lagrangians for quark and lepton sector are given by

$$\begin{aligned}
-\mathcal{L}_L = \sum_{\ell=e,\mu,\tau} & [y_\ell \bar{L}_{L_\ell} \Phi \ell_R + y_{S_\ell} \bar{L}_{L_\ell} L'_{R_\ell} S + M_\ell \bar{L}'_{L_\ell} L'_{R_\ell}] \\
& + y_{\Delta_1} \bar{L}_{L_e}^C (i\sigma_2) \Delta L'_{L_e} + y_{\Delta_2} \bar{L}_{L_\tau}^C (i\sigma_2) \Delta L'_{L_\mu} + y_{\Delta_3} \bar{L}_{L_\mu}^C (i\sigma_2) \Delta L'_{L_\tau} \\
& + y_{E_1} \varphi^* \bar{L}'_{L_e} L'_{R_\mu} + y_{E_2} \varphi \bar{L}'_{L_e} L'_{R_\tau} + \text{c.c.},
\end{aligned} \tag{II.1}$$

where σ_2 is the second Pauli matrix, and again $L' \equiv [N, E]^T$.

We parametrize the scalar fields as

$$\Phi = \begin{bmatrix} w^+ \\ \frac{v+\phi+iz}{\sqrt{2}} \end{bmatrix}, \quad \Delta = \begin{bmatrix} \frac{\Delta^+}{\sqrt{2}} & \Delta^{++} \\ \Delta^0 & -\frac{\Delta^+}{\sqrt{2}} \end{bmatrix}, \quad \Delta_0 = \frac{\Delta_R + i\Delta_I}{\sqrt{2}}, \quad \varphi = \frac{v' + \rho + iz'}{\sqrt{2}} \tag{II.2}$$

where $v \simeq 246$ GeV is VEV of the Higgs doublet, and w^\pm , z , and z' are respectively GB which are absorbed by the longitudinal component of W , Z , and $Z'(\equiv Z_{\mu-\tau})$ boson. Then we have two neutral boson mass matrices $m_{\rho\phi}^2$ and $m_{S\Delta}^2$ in the basis of $[\rho, \phi]^T$ and $[S, \Delta_R]^T$, and these are diagonalized by $O_a^T m_{\rho\phi}^2 O_a \equiv \text{Diag}[m_{h_1}, m_{h_2}]$ and $O_\alpha^T m_{S\Delta}^2 O_\alpha \equiv \text{Diag}[m_{H_1}, m_{H_2}]$ respectively, where the mixing source of O_α arises from the nontrivial quartic coupling $\lambda_0 \Phi^T (i\sigma_2) \Delta^\dagger \Phi S$ and each of mass eigenstate can be written in terms of couplings of Higgs potential². Here we define mixing matrices as

$$O_{a(\alpha)} = \begin{bmatrix} c_{a(\alpha)} & s_{a(\alpha)} \\ -s_{a(\alpha)} & c_{a(\alpha)} \end{bmatrix}, \quad s_a = \frac{2\lambda_{\Phi\varphi}}{m_{h_1}^2 - m_{h_2}^2}, \quad s_\alpha = \frac{2\sqrt{2}\lambda_0}{m_{H_1}^2 - m_{H_2}^2}, \tag{II.3}$$

where $c(s)_{a(\alpha)}$ is the short-hand notation of $\cos(\sin)_{a(\alpha)}$. Notice here that we suppose to be $O_a \approx 1$ below analysis, which could however be a natural assumption because $s_a \lesssim 0.2$ from the LHC experiment, therefore $m_\rho \approx m_{h_1}$ and $m_\phi \approx m_{h_2}$.

² See Appendix in details.

After the $\mu - \tau$ gauge symmetry breaking, *vector-like fermion mass matrix* can be written in the basis $[L'_e, L'_\mu, L'_\tau]^T$ as follows:

$$M_{L'} \equiv \begin{bmatrix} M_e & M_{e\mu} & M_{e\tau} \\ M_{e\mu} & M_\mu & 0 \\ M_{e\tau} & 0 & M_\tau \end{bmatrix}, \quad (\text{II.4})$$

where we simply assume to be positive real for each component and define $M_{e\mu} \equiv y_{E1} v' / \sqrt{2}$ and $M_{e\tau} \equiv y_{E2} v' / \sqrt{2}$. Then $M_{L'}$ is diagonalized by orthogonal mixing matrix V ($VV^T = 1$) as

$$V^T M_{L'} V = D_N \equiv [M_1, M_2, M_3], \quad N_{e,\mu,\tau} = V N_{1,2,3}, \quad (\text{II.5})$$

where $M_{1,2,3}$ is the mass eigenstate.

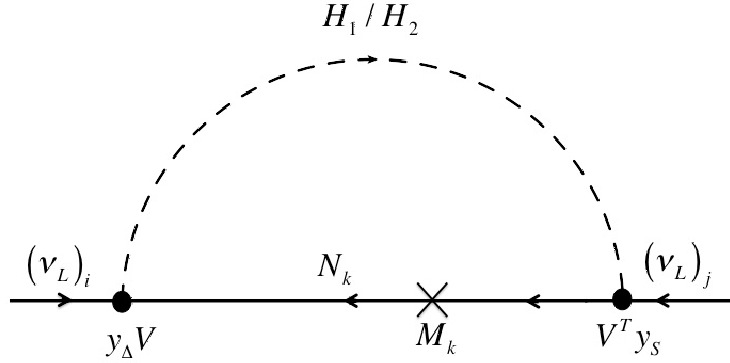


FIG. 1: The Feynman diagram for generating neutrino mass matrix.

A. Active neutrino mass and lepton flavor violating processes

Our *active neutrino mass matrix* is given in general at one-loop level by the diagram shown in Fig. 1 which is calculated as [17]

$$m_\nu = y_\Delta \epsilon V M R V^T y_S + [y_\Delta \epsilon V M R V^T y_S]^T, \quad (\text{II.6})$$

$$\epsilon \equiv \begin{bmatrix} 1 & 0 & 0 \\ 0 & 0 & 1 \\ 0 & 1 & 0 \end{bmatrix}, \quad R_k = \frac{s_\alpha c_\alpha}{(4\pi)^2} \left[\frac{r_{k2} \ln r_{k2}}{1 - r_{k2}} - \frac{r_{k1} \ln r_{k1}}{1 - r_{k1}} \right], \quad (\text{II.7})$$

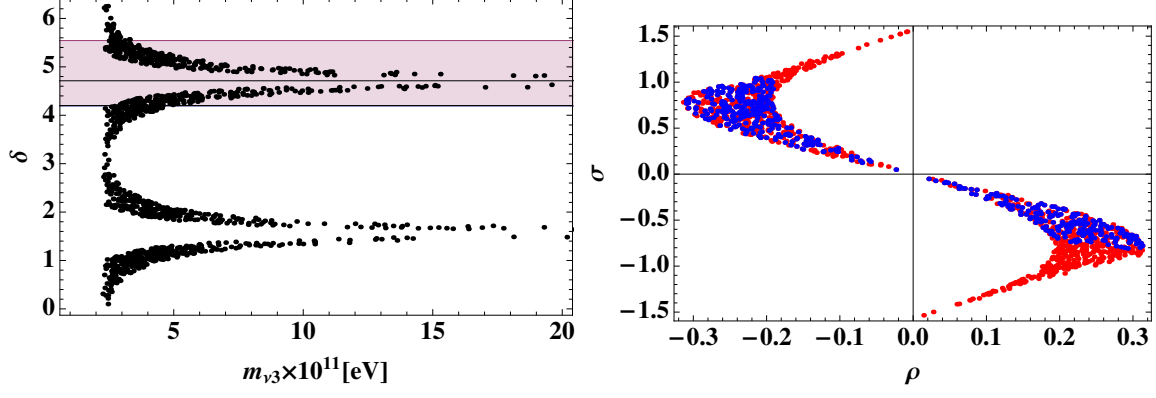


FIG. 2: The right side of figure represents correlation between m_{ν_3} and δ which is Dirac phase, while the right side of figure represents correlation between ρ and σ which are Majorana phases. Here the pink region in the left side figure is given by $\delta = [-2.09, -0.74]$ at 90 % confidential level with the best fit value $\delta \approx -\pi/2$, and the blue points in the right side figure correspond to the parameter sets providing the points in the pink region.

where $r_{k_a} \equiv (m_{H_a}/M_k)^2$, y_S and y_Δ are diagonal Yukawa matrices respectively. Then the neutrino mass is diagonalized by 3 by 3 unitary matrix U as $m_\nu = UD^\nu U^T$, where $D^\nu \equiv \text{diag.}[m_{\nu_1}e^{2i\rho}, m_{\nu_2}e^{2i\sigma}, m_{\nu_3}]$ is neutrino mass eigenvalues [18]. Applying Eq. (II.6) and an arbitral complex anti-symmetric matrix A to $m_\nu = UD^\nu U^T$, one finds a relation $y_\Delta \epsilon V M R V^T y_S = (UD^\nu U^T + A)/2$ [17].

In order to obtain some predictions to the neutrino sector here, we impose an assumption $M \equiv M_1 \approx M_2 \approx M_3$. Then m_ν is simplified as

$$\begin{aligned}
 m_\nu &\approx R [y_\Delta \epsilon (V M V^T) y_S + y_S (V M V^T) \epsilon y_\Delta] \\
 &= R (y_\Delta \epsilon M_{L'} y_S + y_S M_{L'} \epsilon y_\Delta) \\
 &= R \begin{bmatrix} 2M_e y_{S_e} y_{\Delta_1} & M_{e\tau} y_{S_e} y_{\Delta_2} + M_{e\mu} y_{S_\mu} y_{\Delta_1} & M_{e\mu} y_{S_e} y_{\Delta_3} + M_{e\tau} y_{S_\tau} y_{\Delta_1} \\ M_{e\tau} y_{S_e} y_{\Delta_2} + M_{e\mu} y_{S_\mu} y_{\Delta_1} & 0 & M_{\mu} y_{S_\mu} y_{\Delta_3} + M_{\tau} y_{S_\tau} y_{\Delta_2} \\ M_{e\mu} y_{S_e} y_{\Delta_3} + M_{e\tau} y_{S_\tau} y_{\Delta_1} & M_{\mu} y_{S_\mu} y_{\Delta_3} + M_{\tau} y_{S_\tau} y_{\Delta_2} & 0 \end{bmatrix} \quad (\text{II.8})
 \end{aligned}$$

$$\approx \begin{bmatrix} 0.022 - 0.75 & 0.028 - 0.039 & 0.030 - 0.040 \\ 0.028 - 0.039 & 0 & 0.023 - 0.75 \\ 0.030 - 0.040 & 0.023 - 0.75 & 0 \end{bmatrix} [\text{eV}], \quad (\text{II.9})$$

where we have used $VMV^T = VV^T M_{L'} VV^T = M_{L'}$. Eq. (II.8) corresponds to the type C two zero texture that provides several predictions that only an inverted neutrino mass ordering is allowed and specific pattern of δ in the right side of fig. 2³ and specific Majorana phases (ρ, σ) in the right side of fig. 2 are obtained, where we adapt the recent global neutrino oscillation data [19] up to 3σ confidential level in the section of numerical analysis. We find that the region of σ is restricted when the Dirac phase is within $\delta = [-2.09, -0.74]$ which is 90% confidence level range with the best fit value $\delta \sim -\pi/2$. We obtain these numerical values of the last Eq. (II.9) by using their central values of neutrino oscillation data.

In the numerical analysis below, we will show this prediction combined with the other phenomenologies such as LFVs and DM

Lepton flavor violations (LFVs) arises from the term y_Δ and y_S at one-loop level, and its form can be given by

$$\text{BR}(\ell_i \rightarrow \ell_j \gamma) = \frac{48\pi^3 \alpha_{\text{em}} C_{ij}}{G_F^2 m_{\ell_i}^2} (|a_{R_{ij}}|^2 + |a_{L_{ij}}|^2), \quad (\text{II.10})$$

$$a_{R_{ij}} = \frac{1}{(4\pi)^2} \sum_{k=1,2,3} \left[\frac{Y_{\Delta_{ki}}^\dagger Y_{\Delta_{jk}}}{2} (m_{\ell_j} F_2[M_k, m_{\Delta^\pm}] + 2m_{\ell_i} (2F_2[M_k, m_{\Delta^{\pm\pm}}] + F_2[m_{\Delta^{\pm\pm}}, M_k])) \right. \\ \left. - Y_{S_{ki}}^\dagger Y_{S_{jk}} m_{\ell_i} (c_\alpha^2 F_2[H_1, M_k] + s_\alpha^2 F_2[H_2, M_k]) \right], \quad (\text{II.11})$$

$$a_{L_{ij}} = \frac{1}{(4\pi)^2} \sum_{k=1,2,3} \left[\frac{Y_{\Delta_{ki}}^\dagger Y_{\Delta_{jk}}}{2} (m_{\ell_i} F_2[M_k, m_{\Delta^\pm}] + 2m_{\ell_j} (2F_2[M_k, m_{\Delta^{\pm\pm}}] + F_2[m_{\Delta^{\pm\pm}}, M_k])) \right. \\ \left. - Y_{S_{ki}}^\dagger Y_{S_{jk}} m_{\ell_j} (c_\alpha^2 F_2[H_1, M_k] + s_\alpha^2 F_2[H_2, M_k]) \right], \quad (\text{II.12})$$

$$F_2(m_a, m_b) = \frac{2m_a^6 + 3m_a^4 m_b^2 - 6m_a^2 m_b^4 + 6m_b^6 + 12m_a^4 m_b^2 \ln(m_b/m_a)}{12(m_a^2 - m_b^2)^4}, \quad (\text{II.13})$$

where η^\pm is the singly charged component of η , $G_F \approx 1.17 \times 10^{-5} [\text{GeV}]^{-2}$ is the Fermi constant, $\alpha_{\text{em}} \approx 1/137$ is the fine structure constant, $C_{21} \approx 1$, $C_{31} \approx 0.1784$, and $C_{32} \approx 0.1736$. Experimental upper bounds are respectively given by $\text{BR}(\mu \rightarrow e \gamma) \lesssim 4.2 \times 10^{-13}$, $\text{BR}(\tau \rightarrow e \gamma) \lesssim 3.3 \times 10^{-8}$, and $\text{BR}(\tau \rightarrow \mu \gamma) \lesssim 4.4 \times 10^{-8}$.

New contributions to the muon anomalous magnetic moment (muon $g-2$: Δa_μ) arises from Yukawa terms y_Δ with negative contribution and y_S with positive contribution. Also another

³ The recent data of T2K [20] suggests $\delta \approx -\pi/2$, therefore the maximum value of $m_{\nu_3} \approx \mathcal{O}(0.1) \text{eV}$ is in favored in our model.

source via additional gauge sector can also be induced by

$$\Delta a_\mu = \Delta a_\mu^{Yukawa} + \Delta a_\mu^{Z'}, \quad (\text{II.14})$$

$$\Delta a_\mu^{Yukawa} = -m_\mu [a_R + a_L]_{\mu\mu}, \quad \Delta a_\mu^{Z'} \approx \frac{g_{Z'}^2}{8\pi^2} \int_0^1 da \frac{2ra(1-a)^2}{r(1-a)^2 + a}, \quad (\text{II.15})$$

where $r \equiv (m_\mu/M_{Z'})^2$, and Z' is the new gauge vector boson. Thus we could explain the sizable muon $g-2$ ($\approx \mathcal{O}[10^{-9}]$) [21], if we can satisfy the constraint of trident process. Notice here that $g_{Z'} \lesssim 10^{-3}$ [22] has to be satisfied due to the trident process, and we use the allowed range $10^{-9} \lesssim \Delta a_\mu \lesssim 4 \times 10^{-9}$ in our numerical analysis below.

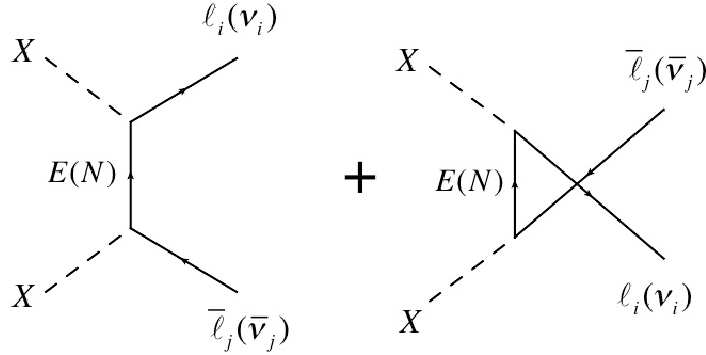


FIG. 3: The dominant DM annihilation processes.

B. Dark matter

Here we consider the lightest inert boson $X \equiv H_1$, and assume to neglect $s_\alpha \ll 1$ and any Higgs couplings to simply evade the constraint of direct detection searches through Higgs portal. In this case, dominant DM annihilation processes are $XX \rightarrow \ell_i \bar{\ell}_j (\nu_i \bar{\nu}_j)$ via Yukawa interactions associated with Yukawa couplings y_S and y_Δ , which are shown in Fig. 3. Then the non-relativistic cross section to explain the relic density of DM is d -wave dominant, and its effective form is given by

$$d_{\text{eff}} \approx \sum_{i,j,k}^{1-3} \frac{s_\alpha^4 |(Y_\Delta)_{ki}^\dagger (Y_\Delta)_{jk}|^2 + 2c_\alpha^4 |(Y_S)_{ki}^\dagger (Y_S)_{jk}|^2}{60\pi(1+r_k)^4 M_X^2} \approx \frac{1}{30\pi M_X^2} \sum_{i,j,k}^{1-3} \frac{|(Y_S)_{ki}^\dagger (Y_S)_{jk}|^2}{(1+r_k)^4}, \quad (\text{II.16})$$

where $r_k \equiv (M_k/M_X)^2$. Then the relic density Ωh^2 is simply given by [23]

$$\Omega h^2 \approx \frac{10.7 \times 10^9 x_f^3}{20\sqrt{g_*} M_P d_{\text{eff}}}, \quad (\text{II.17})$$

where $M_P \approx 1.22 \times 10^{19} [\text{GeV}]$ is the Planck mass, $g_* \approx 100$ is the total number of effective relativistic degrees of freedom at the time of freeze-out, and $x_f \approx 25$ is defined by M_X/T_f at the freeze out temperature (T_f). The measured relic density is reported by Planck that suggests $\Omega h^2 \approx 0.12$ [24]. In our numerical analysis below, however, we will adopt more relaxed value $0.11 \lesssim \Omega h^2 \lesssim 0.13$.

III. NUMERICAL ANALYSIS

In this section, we show a global analysis, where we have fixed some parameters for simplicity. At first, we fix $m_{H_2} = m_{\Delta^\pm} = m_{\Delta^{\pm\pm}}$ in order to evade the oblique parameters in the triplet boson. We also fix these three degenerated mass eigenvalues and corresponding rotation matrix used for diagonalizing $M_{L'}$ as follows:

$$M \equiv M_1 \approx M_2 \approx M_3 \approx 1700 [\text{GeV}], \quad V \approx \begin{bmatrix} 0.707 & -0.707 & -0.000232 \\ -0.412 & 0.413 & 0.812 \\ -0.574 & -0.574 & -0.583 \end{bmatrix}. \quad (\text{III.1})$$

Then we randomly select the following range of input parameters as

$$M_X \in [900, 2000] [\text{GeV}], \quad M_{Z'} \in [10^{-3}, 10^3] [\text{GeV}], \quad m_{H_2} \in [1.2M_X, 2500] [\text{GeV}], \\ |y_{S_e}| \in [0.1, 4\pi], \quad |y_{S_\tau}| \in [0.1, 4\pi], \quad |s_\alpha| \in [10^{-5}, 0.1], \quad g_{Z'} \in [10^{-5}, 10^{-3}], \quad (\text{III.2})$$

where the lower bound $M_X = 900 \text{ GeV}$ originates from the relic density of DM, Yukawa couplings y_Δ and y_{S_μ} can be rewritten in terms of $M_{L'}$, R , and neutrino oscillation data in Eqs. (II.8) and (II.9), where we have used the central value of Eq. (II.9). Then we explore the allowed region to satisfy all the constraints such as neutrino oscillation, LFVs, muon $g - 2$, and relic density of DM as discussed above.

In the numerical analysis, we firstly find that the Yukawa contribution to the muon $g - 2$ $\Delta a_\mu^{\text{Yukawa}}$ is at most the order of $\mathcal{O}(10^{-16})$, therefore $\Delta a_\mu \approx \Delta a_\mu^{Z'}$. In this case, notice here that we have to consider the constraint from neutrino trident production process [22]. This is because we take $g_{Z'} \lesssim 10^{-3}$ as discussed in the last part of muon $g - 2$. In the left side of fig. 4, we show the allowed region to satisfy all the data in terms of $g_{Z'}$ and $M_{Z'}$, and its form directly reflects Eq. (II.15). And this figure provide the upper bound on $M_{Z'} \lesssim 0.2$.

While the right side of fig. 4 represents the allowed region to satisfy all the data in terms of M_X and m_{H_2} , and it suggests all the region that we take are allowed.

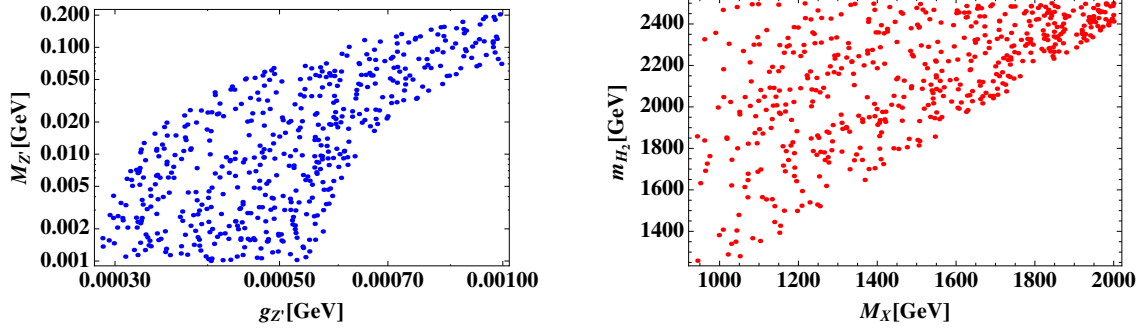


FIG. 4: In the left side of fig. 4, we show the allowed region to satisfy all the data in terms of $g_{Z'}$ and $M_{Z'}$, and its form directly reflects Eq. (II.15). And this figure provide the upper bound on $M_{Z'} \lesssim 0.2$. While the right side of fig. 4 represents the allowed region to satisfy all the data in terms of M_X and m_{H_2} , and it suggest all the region that we take are allowed.

IV. CONCLUSIONS AND DISCUSSIONS

We have proposed an predictive radiative seesaw model at one-loop level with a flavor dependent gauge symmetry $U(1)_{\mu-\tau}$, in which we have consider gauge singlet -like bosonic dark matter candidate. And we have obtained a specific two zero texture (type-C) of active neutrino mass matrix that provides us several predictions such as inverted mass ordering, specific pattern of Dirac CP phase and Majorana phases. Here we have assumed that three of exotic fermion masses are almost degenerated, which is an minimal requirement to obtain such a specific neutrino texture.

We have also carried out a numerical analysis to search for parameter region which satisfy all the experimental data such as constraints from charged lepton flavor violations, sizable muon $g-2$, relic density of dark matter, as well as neutrino oscillation data. In this analysis, we have firstly found that $\Delta a_\mu^{Yukawa} \approx \mathcal{O}(10^{-16})$ is negligible compared to the measured value $\mathcal{O}(10^{-9})$, therefore $\Delta a_\mu \approx \Delta a_\mu^{Z'}$.

In the left side of fig. 4, we have shown the allowed region to satisfy all the data in terms of $g_{Z'}$ and $M_{Z'}$, and its form directly reflects Eq. (II.15). And this figure provide the upper

bound on $M_{Z'} \lesssim 0.2$. While the right side of fig. 4 has represented the allowed region to satisfy all the data in terms of M_X and m_{H_2} , and it suggests all the region that we have taken are allowed.

In our model, we have inert doubly charged Higgs boson which decay into dark matter and SM fermions by cascade decay modes. It will be interesting to search for the signal of "missing E_T + same sign leptons" as a signature of the inert Higgs triplet as well as our dark matter. The detailed analysis of the signal is beyond the scope of this paper and it will be studied elsewhere.

Appendix

Here we give the most general Higgs potential in a renormalizable theory as

$$\begin{aligned}
\mathcal{V} = & m_\Phi^2 \Phi^\dagger \Phi + m_\varphi^2 \varphi^* \varphi + m_\Delta^2 \text{Tr}[\Delta^\dagger \Delta] + m_S^2 S^2 \\
& + (\lambda_0 \Phi^T (i\sigma_2) \Delta^\dagger \Phi S + \text{c.c.}) + \lambda_\Phi |\Phi^\dagger \Phi|^2 + \lambda_\varphi |\varphi^* \varphi|^2 + \lambda_\Delta (\text{Tr}[\Delta^\dagger \Delta])^2 + \lambda'_\Delta \text{Det}[\Delta^\dagger \Delta] + \lambda_S S^4 \\
& + \lambda_{\Phi\varphi} (\Phi^\dagger \Phi) (\varphi^* \varphi) + \lambda_{\Phi\Delta} (\Phi^\dagger \Phi) \text{Tr}[\Delta^\dagger \Delta] + \lambda'_{\Phi\Delta} \sum_{i=1-3} (\Phi^\dagger \tau_i \Phi) \text{Tr}[\Delta^\dagger \tau_i \Delta] + \lambda_{\Phi S} (\Phi^\dagger \Phi) S^2 \\
& + \lambda_{\varphi\Delta} \varphi^* \varphi \text{Tr}[\Delta^\dagger \Delta] + \lambda_{\varphi S} \varphi^* \varphi S^2 + \lambda_{\Delta S} \text{Tr}[\Delta^\dagger \Delta] S^2.
\end{aligned} \tag{IV.1}$$

Acknowledgments

H. O. is sincerely grateful for all the KIAS members, Korean cordial persons, foods, culture, weather, and all the other things.

-
- [1] A. Crivellin, G. D'Ambrosio and J. Heeck, Phys. Rev. D **91**, no. 7, 075006 (2015) [arXiv:1503.03477 [hep-ph]].
 - [2] C. Kownacki, E. Ma, N. Pollard and M. Zakeri, arXiv:1611.05017 [hep-ph].
 - [3] X. G. He, G. C. Joshi, H. Lew and R. R. Volkas, Phys. Rev. D **43**, 22 (1991); D **44**, 2118 (1991).
 - [4] S. Baek, N. G. Deshpande, X. G. He and P. Ko, Phys. Rev. D **64**, 055006 (2001) [hep-ph/0104141].

- [5] E. Ma, D. P. Roy and S. Roy, Phys. Lett. B **525**, 101 (2002) [hep-ph/0110146].
- [6] E. J. Chun and K. Turzynski, Phys. Rev. D **76**, 053008 (2007) [hep-ph/0703070].
- [7] S. Baek and P. Ko, JCAP **0910**, 011 (2009) [arXiv:0811.1646 [hep-ph]].
- [8] K. Harigaya, T. Igari, M. M. Nojiri, M. Takeuchi and K. Tobe, JHEP **1403**, 105 (2014) [arXiv:1311.0870 [hep-ph]].
- [9] W. Altmannshofer, S. Gori, M. Pospelov and I. Yavin, Phys. Rev. D **89**, 095033 (2014) [arXiv:1403.1269 [hep-ph]].
- [10] J. Heeck, M. Holthausen, W. Rodejohann and Y. Shimizu, Nucl. Phys. B **896**, 281 (2015) [arXiv:1412.3671 [hep-ph]].
- [11] T. Araki, F. Kaneko, Y. Konishi, T. Ota, J. Sato and T. Shimomura, Phys. Rev. D **91**, no. 3, 037301 (2015) [arXiv:1409.4180 [hep-ph]].
- [12] S. Baek, H. Okada and K. Yagyu, JHEP **1504**, 049 (2015) [arXiv:1501.01530 [hep-ph]].
- [13] T. Araki, F. Kaneko, T. Ota, J. Sato and T. Shimomura, Phys. Rev. D **93**, no. 1, 013014 (2016) [arXiv:1508.07471 [hep-ph]].
- [14] S. Baek, Phys. Lett. B **756**, 1 (2016) [arXiv:1510.02168 [hep-ph]].
- [15] P. Ko, T. Nomura and H. Okada, arXiv:1701.05788 [hep-ph].
- [16] P. Ko, T. Nomura and H. Okada, arXiv:1702.02699 [hep-ph].
- [17] H. Okada and Y. Orikasa, Phys. Rev. D **94**, no. 5, 055002 (2016) [arXiv:1512.06687 [hep-ph]].
- [18] H. Fritzsch, Z. z. Xing and S. Zhou, JHEP **1109**, 083 (2011) [arXiv:1108.4534 [hep-ph]].
- [19] D. V. Forero, M. Tortola and J. W. F. Valle, Phys. Rev. D **90**, no. 9, 093006 (2014) [arXiv:1405.7540 [hep-ph]].
- [20] Talk by Konosuke Iwamoto (T2K Collaboration) at the ICHEP 2016, Chicago, August 2016.
- [21] G. W. Bennett *et al.* [Muon G-2 Collaboration], Phys. Rev. D **73**, 072003 (2006) [hep-ex/0602035].
- [22] W. Altmannshofer, S. Gori, M. Pospelov and I. Yavin, Phys. Rev. Lett. **113**, 091801 (2014) [arXiv:1406.2332 [hep-ph]].
- [23] M. Srednicki, R. Watkins and K. A. Olive, Nucl. Phys. B **310**, 693 (1988).
- [24] P. A. R. Ade *et al.* [Planck Collaboration], Astron. Astrophys. **571**, A16 (2014) [arXiv:1303.5076 [astro-ph.CO]].